A Luminescent Complex of Europium and Tetracycline Labels Liquid Disordered Membrane Domains and Causes GM1 Redistribution

Jennie L. Cawley[a], Ariana I. McDarby[a,1], Aurelia R. Honerkamp-Smith[b] and Nathan J. Wittenberg[a,*]

[a]Department of Chemistry, Lehigh University, 6 East Packer Avenue, Bethlehem, PA,18015, USA.

[b]Department of Physics, Lehigh University, 17 Memorial Drive East, Bethlehem, PA, 18015, USA.

[1]Present Address: Department of Chemistry and Biochemistry, North Dakota State University, Dept. 2735, PO Box 6050 Fargo, North Dakota, 58108, USA

*Corresponding Author: Department of Chemistry, Lehigh University, 6 East Packer Avenue, Bethlehem, PA, USA. ORCID: 0000-0001-9196-1867. Email: njw@lehigh.edu

ABSTRACT

Microdomains in lipid bilayer membranes are routinely imaged using organic fluorophores that preferentially partition into one of the lipid phases, resulting in fluorescence contrast. Here we show that membrane microdomains in giant unilamellar vesicles (GUVs) can be visualized with europium luminescence using a complex of europium (III) and tetracycline (EuTc). EuTc is unlike typical organic lipid probes in that it has a unique excitation/emission wavelength combination (396/617 nm), a very large Stokes shift (221 nm), and a very narrow emission bandwidth (8 nm). The probe preferentially interacts with liquid disordered domains in GUVs, which results in intensity contrast across the surface of phase-separated GUVs. Interestingly, EuTc also disrupts GM1 partitioning. After labeling phase-separated GUVs with EuTc, CTxB, which binds GM1, labels disordered domains. We hypothesize that this is due to the ability of EuTc to increase lipid membrane order, which we demonstrate by showing that EuTc significantly reduces lipid diffusion coefficients. We conclude that EuTc, and potentially other tetracycline derivatives complexed with metal ions, disrupt membrane organization of lipid bilayer membranes, which may have implications on the antibacterial activity of the tetracycline family of antibiotics.

KEYWORDS: Giant unilamellar vesicles, lipid membranes, membrane microdomains, luminescence, fluorescence, europium, tetracycline, GM1

INTRODUCTION

Characterizing lipid membrane spatial heterogeneity is essential to understanding the structure and function of cellular membranes. Cell membranes are asymmetric and may be organized into dynamic, laterally-heterogeneous nanometer-sized membrane domains known as "lipid rafts." Lipid rafts contain a variety of lipids and proteins involved in cell signaling processes.[1] Due to the complexity of cell membranes, many researchers turn to model membranes, such as liposomes, giant unilamellar vesicles (GUVs), or supported lipid bilayers (SLBs). Model membranes are advantageous because they mimic cellular membranes and their composition can be tightly controlled. Model membranes can possess raft-like liquid ordered (Lo) domains that are enriched in saturated phospholipids, sphingolipids, cholesterol and glycosphingolipids, like gangliosides.[2,3] A second phase, referred to as the liquid disordered (Ld) domain is enriched in unsaturated lipids. The most common strategy for imaging Lo and Ld domains is fluorescence microscopy, which is typically accomplished by incorporating lipid-conjugated organic fluorophores or polycyclic aromatic hydrocarbons that partition into one phase or the other.[4,5] Conveniently, these probes are often compatible with "off-the-shelf" filter cubes; however, they have small Stokes shifts and broad emission spectra resulting in fluorescence crosstalk that limits image multiplexing possibilities.

To overcome these limitations and expand the membrane imaging toolbox, we utilize a luminescent complex composed of europium III (Eu^{3+}) and tetracycline (Tc) to identify membrane phase heterogeneity among giant unilamellar vesicles (GUVs). Lanthanide luminescence, including Eu^{3+}, has been exploited for many biological imaging applications,[6–11] and here we show that a simple ligand, Tc, enables the imaging of lipid membrane spatial heterogeneity. The luminescence of Eu^{3+} is enhanced by Tc excitation.[12,13] Tc acts as an antenna, and its excitation is followed by a ligand-to-metal charge transfer, yielding sharp Eu^{3+}

emission bands with the most intense band between 610 and 620 nm. The emission band of EuTc is very narrow in comparison to traditional organic fluorophores. In pure water, the luminescence of EuTc reaches a maximum when the stoichiometry reaches a 1:1 ratio of Eu^{3+}:Tc, suggesting a 1:1 stoichiometry of the complex.[12] The luminescence of the EuTc complex is sensitive to its environment (e.g. pH, hydration shell, other ligands).[13] Analytes that can enter the Eu^{3+} inner coordination sphere displace water.[14,15] Coordinated water quenches some EuTc emission by accepting energy from the excited Eu^{3+} states followed by non-radiative decay.[16] Therefore, displacement of water from the inner coordination sphere causes a significant increase in emission intensity. Due to this phenomenon, the EuTc complex has been applied to the detection of LDL cholesterol, various surfactants, DNA, hydrogen peroxide, and sialic acid-bearing cancer biomarkers in human plasma.[7,14,17–21] In all cases, the EuTc complex proved to be highly sensitive for the analyte of interest. It also is a suitable alternative to traditional organic fluorescent probes because it is simply prepared, decomposes slowly, has a working pH of ~7, is fluorescent in buffered systems, and can be used for sensing in dynamic biological systems.[8–10] Considering these advantages and its unique spectral properties, we suspected that EuTc luminescence is sensitive to phospholipid membranes and can be used for membrane imaging. Here we show that EuTc can be used to visualize membrane heterogeneity in GUVs. Finally, we show that EuTc preferentially labels Ld domains, increases membrane order, and surprisingly causes GM_1 redistribution into Ld domains. The interesting redistribution of GM_1 by EuTc may have implications for how metal complexes of Tc (and derivatives) interact with biological membranes in vivo.

2. RESULTS AND DISCUSSION

2.1 EuTc Spectral Characteristics and Lipid Sensitivity

To demonstrate that the EuTc complex is an attractive fluorescent probe for lipid membranes, we compared the excitation and emission characteristics of EuTc and Texas Red-DHPE (TR-DHPE), when associated with DOPC liposomes in 3-morpholinopropane-1-sulfonic acid (MOPS) buffer, pH 7.0. TR-DHPE is a commonly used probe for membrane phase separation that partitions into the Ld phase.[5] As shown in Figure 1a, the excitation maximum for EuTc and TR-DHPE are 396 nm, and 589 nm, respectively. There are two major emission peaks of the EuTc complex centered at 592 nm and 617 nm, which correspond to the $^5D_0 \rightarrow {}^7F_1$ and $^5D_0 \rightarrow {}^7F_2$ transitions of Eu^{3+}, respectively.[14] The sharp EuTc emission peak at 617 nm has a very narrow bandwidth, especially when compared to traditional organic fluorophores. Specifically, the 617 nm emission peak of EuTc has a full width at half maximum (FWHM) of 8 nm, and it is red-shifted 221 nm from the excitation maximum. For comparison, the TR-DHPE emission peak has a FWHM of 32 nm with a Stokes shift of only 20 nm. Figure 1b displays that in the absence of the ligand, Tc, Eu^{3+} luminescence is negligible in the presence of DOPC liposomes. This is expected as free Eu^{3+} has a small molar absorptivity ($\varepsilon < 1\ M^{-1}\ cm^{-1}$)[22] because the pertinent electronic transitions are forbidden.[23]

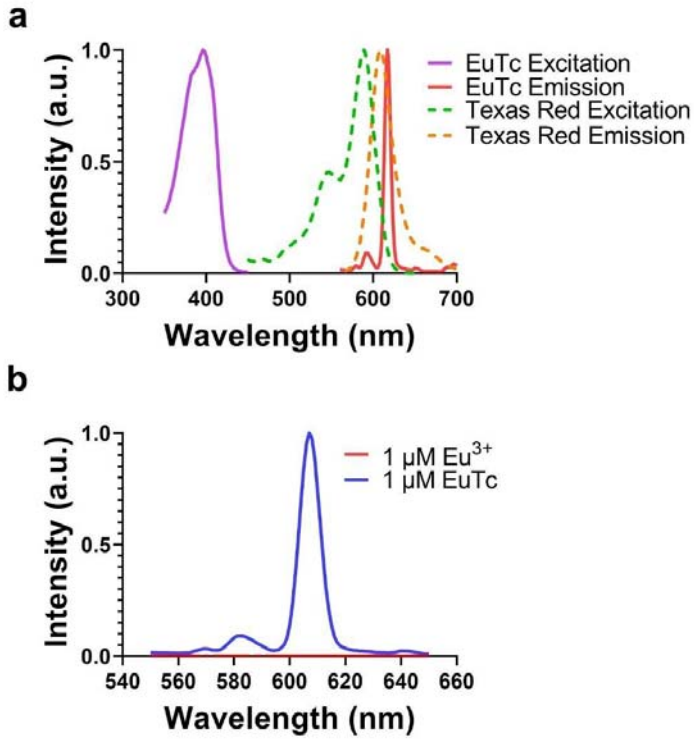

Figure 1. Spectroscopic characteristics of EuTc (1 μM) and Texas Red-DHPE with DOPC liposomes. (a) Excitation and emission of spectra of EuTc compared with excitation and emission spectra of Texas-Red DHPE. (b) Emission spectra of the EuTc complex (1 μM) and Eu^{3+} (1 μM) alone in the presence of DOPC liposomes. EuTc and Eu^{3+} were excited at 400 nm.

Next, we sought to determine if EuTc emission is enhanced by phospholipids in lamellar lipid structures. Previous research has shown that various surfactants (sodium dodecylsulfate (SDS), cetylpyridinium chloride (CPC), Triton-X 100, Brij 58 and Brij 78), all which form micellar structures, can enhance the emission of EuTc.[20] First, we formed liposomes by a series of freeze-thaw cycles and extrusion through a 100-nm pore filter. The liposomes were then exposed to 1 μM EuTc. The liposomes were composed of DOPC, and the lipid concentration ranged from 10 nM to 100 μM. EuTc emission depended on total lipid concentration, and increased with increasing lipid concentration (Fig. 2). This confirms that EuTc emission is sensitive to the concentration of lipids in lamellar structures in an aqueous environment. The

luminescence of the EuTc complex is known to increase upon displacement of water molecules from the coordination sphere. Our results suggest that EuTc interacts with the lipid bilayer membrane in a manner that diminishes non-radiative decay pathways, similar to that of water displacement.

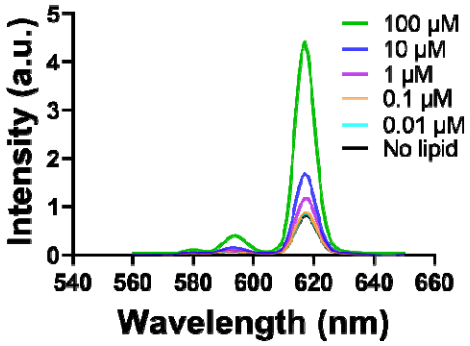

Figure 2. EuTc emission intensity in the presence of DOPC liposomes. The DOPC liposomes enhance EuTc emission intensity in a concentration-dependent manner.

2.2 GUV Imaging with EuTc

In addition to showing that EuTC luminescence is enhanced in the presence of lipids spectroscopically, we sought to demonstrate how the use of the EuTc complex could be used as an imaging probe. To demonstrate this, we prepared single phase (DOPC) and phase separating GUVs (DOPC/DPPC/cholesterol; 40:40:20) and imaged them in the presence of 1 µM EuTc. No other labels were present. For EuTc imaging, a custom filter set was employed (Fig. S1). Labeling DOPC GUVs with EuTc resulted in uniform membrane luminescence, whereas GUVs composed of DOPC/DPPC/cholesterol were heterogeneously labeled (Fig. 3).

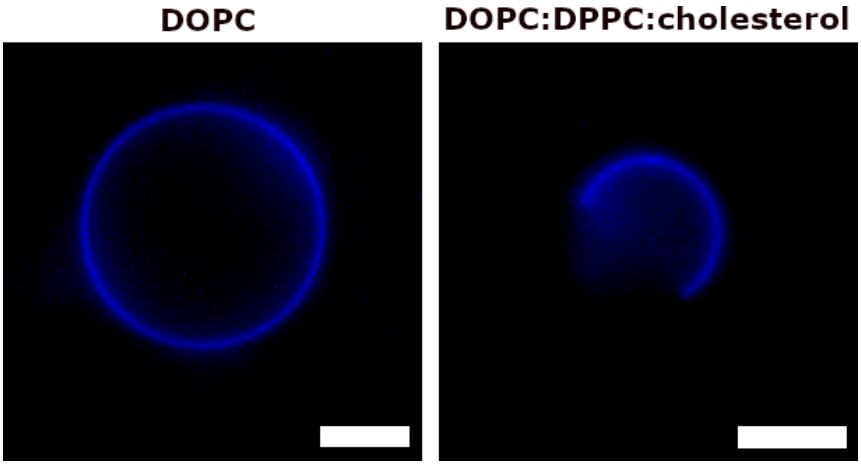

Figure 3. DOPC GUV (left) and a phase separated GUV (DOPC/DPPC/cholesterol, 40:40:20) (right) labeled with 1 μM EuTc. All scale bars are 5 μm.

To explore this further, we prepared additional single phase GUVs with three different lipid compositions: DOPC/cholesterol (80:20), DOPC/GM1 (98:2), and DOPC/GM1/cholesterol (78:2:20).[24,25] GUVs were all presumably in a single liquid phase and were imaged in the presence of 1 μM EuTc, and uniform EuTc luminescence on the membrane was observed (Fig. S2). In addition to the EuTc complex, a fluorescent analog of cholera toxin subunit-B (CTxB-FITC) was added to each imaging chamber containing the GUVs. CTxB-FITC binds GM1 with high affinity[26] and its fluorescence was only observed with GUVs composed of DOPC/GM1 (98:2) and DOPC/GM1/cholesterol (78:2:20). An overlay of EuTc and CTxB-FITC channels display colocalization on the GUV membranes only for GUVs possessing GM1 (Fig. S2). This confirms that EuTc can be used to visualize membranes containing GM1 and/or cholesterol and the presence of the EuTc probe does not appear to significantly alter CTxB-FITC binding to GM1. Interestingly, free Eu^{3+} has been shown to inhibit the binding of complete cholera toxin (A and B subunits) and amyloid-beta oligomers to lipid membranes containing GM1.[27,28] However, we see no evidence that EuTc acts in a similar manner.

As an additional control, single phase GUVs composed of DOPC/GM1/TR-DHPE (98:1:1) were prepared and labeled with CTxB-FITC only. The TR-DHPE and CTxB-FITC signals colocalize on the GUV membrane, as expected (Fig. S3). These results demonstrate the following: first, EuTc is an efficient reporter for visualizing lipid membranes and EuTc labels single phase membranes uniformly, including those containing GM1 and/or cholesterol. Second, EuTc presence does not prevent CTxB-FITC binding to GM1. Third, EuTc can be utilized as a membrane imaging probe and labels phase separating membranes heterogeneously, akin to the well-established TR-DHPE probe.[24] Finally, it is important to note that EuTc was not washed out of the chamber prior to imaging. Despite this, the images have an excellent signal to noise ratio due to the significant luminescence enhancement of EuTc upon its interaction with lipid bilayer membranes. The intensity contrast of EuTc labeling on phase separating GUVs could be explained by two different scenarios. In one scenario, EuTc may preferentially localize with one membrane phase or the other (Ld or Lo). This would increase its local concentration and thus increase the luminescence intensity of that region. Alternatively, EuTc may localize equally to both phases (i.e. equal concentration across both phases), but become more luminescent when interacting with one phase or the other. However, these two scenarios are not mutually exclusive and some combination of them may be responsible for the intensity contrast.

2.3 EuTc Labels Ld Domains and Redistributes GM1

Thus far, we have identified that the EuTc complex can be used as a fluorescent imaging probe for single phase GUVs and labels phase-separated membranes heterogeneously. To determine which phase of the GUV (Ld or Lo) the EuTc probe is labeling, we prepared a series of GUVs with lipid compositions chosen to lie along a tie line in the DOPC-DPPC-cholesterol phase diagram.[2] These compositions yielded vesicles containing different fractions of Lo and

Ld phases with the same composition (Fig. 3, row A). TR-DHPE was included to mark the Ld domains. Upon incubation with EuTc, we observed that the area fraction labeled with EuTc enlarged as the area fraction of the Ld phase increased (Fig. 4, row B). Finally, the TR-DHPE and EuTc signals colocalize (Fig. 4, row C). Taken together, this demonstrates that EuTc labels Ld domains.

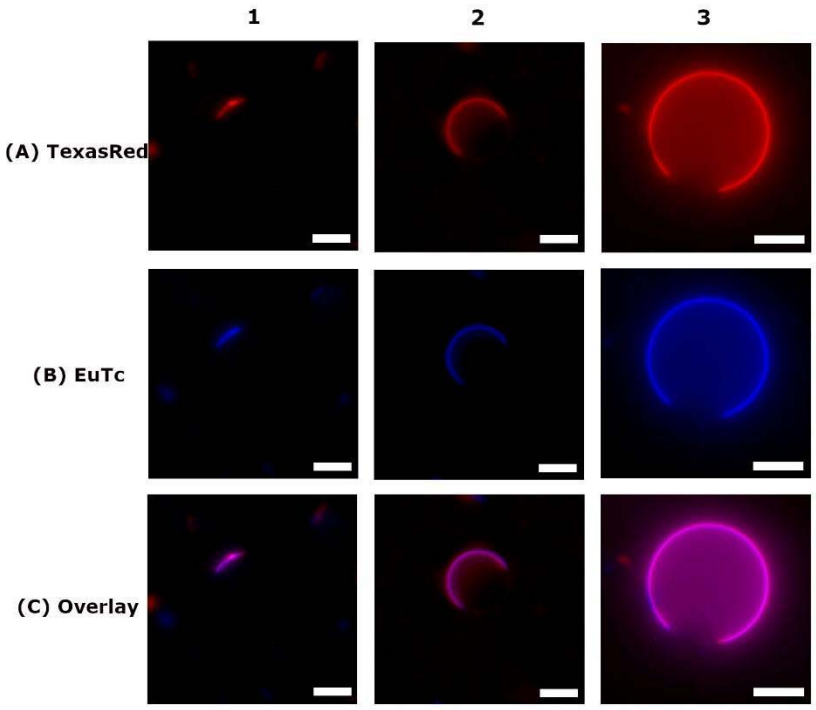

Figure 4. Phase separating GUVs (DOPC, DPPC, cholesterol, and TR-DHPE, varying area fraction of the Ld and Lo phases) imaged by Texas Red (TR-DHPE) and EuTc luminescence. Column labels indicate GUV compositions: (1) DOPC/DPPC/chol/TR-DHPE (19:55:25:1), (2) DOPC/DPPC/chol/TR-DHPE (39.5:39.5:20:1), (3) DOPC/DPPC/chol/TR-DHPE (59:25:15:1), whereas rows indicate fluorescence due to (A) Texas Red and (B) EuTc labeling. Overlay images (C) show colocalization of EuTc and Texas Red on the GUV membrane. All scale bars are 5 µm.

To further confirm that EuTc labels Ld domains, we sought to label Ld and Lo domains concurrently. In this set of experiments, we used CTxB binding to GM1 to label the Lo domains.

GM1 is known to strongly partition into Lo domains in phase separated GUVs,[29] thus binding of GM1 by fluorescent CTxB will indicate the position of the Lo domains. We prepared GUVs composed of DOPC/DPPC/cholesterol/GM1 (39.5:39.5:20:1) and labeled the GUVs first with 10 nM CTxB-Alexa647 and then with 1 μM EuTc. Figure 5, column 1 shows that CTxB-Alexa647 only labels one region of the GUV, which, based on prior precedent, we presume to be the Lo phase. Surprisingly, the EuTc labels the same region of the GUV as CTxB-Alexa647. This is a highly unexpected result because when we prepared phase separating GUVs and labeled them with TR-DHPE, a Ld label, TR-DHPE and EuTc colocalized (Fig 4, Fig. 5, column 4). To evaluate this further, we prepared GUVs in a way in which all labels would be present. These GUVs consisted of DOPC/DPPC/cholesterol/GM1/TR-DHPE, and were exposed to the CTxB-Alexa647 and EuTc labels in a stepwise fashion. The GUVs were exposed to CTxB-Alexa647, imaged, and then subsequently exposed to EuTc and further imaged. Upon the addition of CTxB-Alexa647, we observed that CTxB-Alexa647 and TR-DHPE label oppositely to one another (Figure 5, column 2). It is well established that GM1 partitions into the Lo phase, thus CTxB-Alexa647 is a Lo phase label.[30] Conversely, TR-DHPE is a Ld phase label.[5] Next, we exposed the GUVs to the EuTc complex. Upon imaging the GUVs, we observed that all three labels, EuTc, CTxB-Alexa647, and TR-DHPE colocalize (Fig. 5, column 3). The persistent colocalization of the EuTc and TR-DHPE labels confirm that the CTxB-Alexa647 does not impede TR-DHPE partitioning or EuTc labeling.

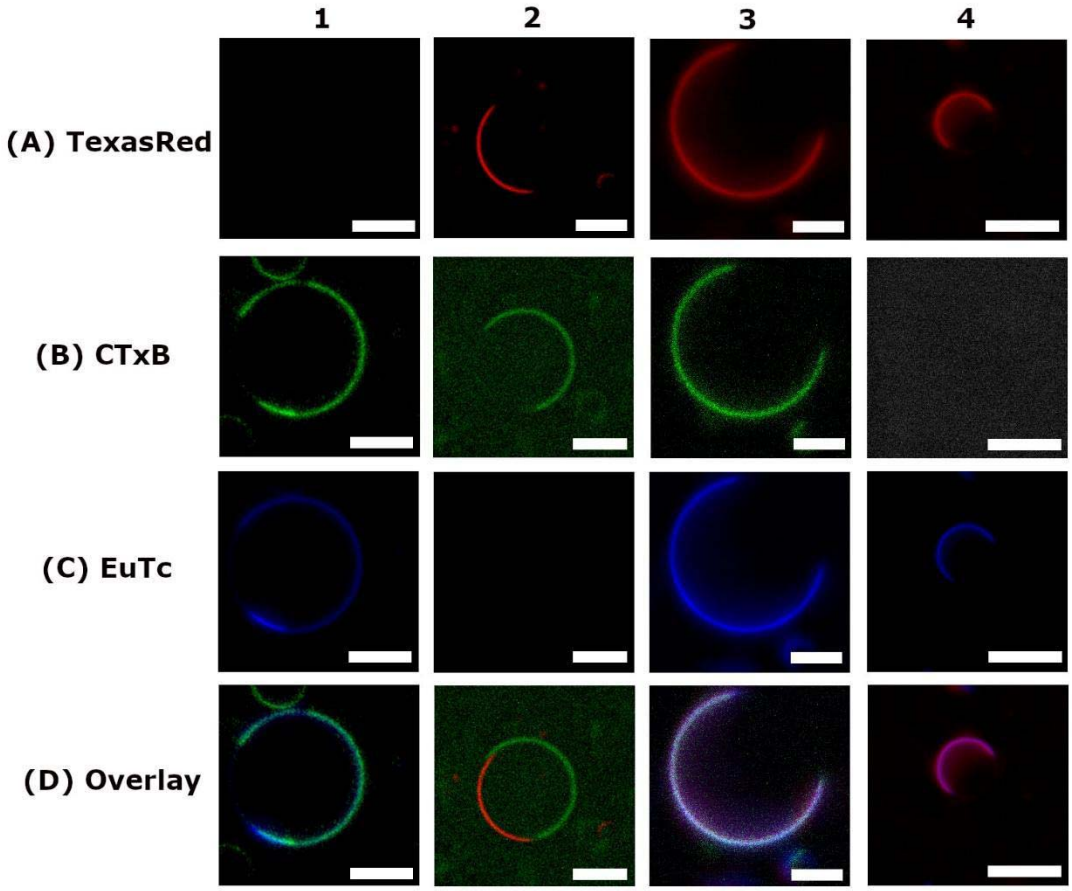

Figure 5. Imaging phase separation in GUVs. Phase separating GUVs imaged by either Texas Red (TR-DHPE) and/or EuTc luminescence and/or CTxB-AlexaFluor647. Column labels indicate GUV composition: (1) DOPC/DPPC/chol/GM1 (39.5:39.5:20:1), (2 and 3) DOPC/DPPC/chol/GM1/TR-DHPE (39:39:20:1:1), (4) DOPC/DPPC/chol/TR-DHPE (39.5:39.5:20:1) whereas rows indicate fluorescence due to (A) Texas Red, (B) CTxB-AlexaFluor647, and (C) EuTc labeling. Overlay images (D) show colocalization of EuTc and Texas Red, EuTC, and CTxB as well as colocalization among EuTC, TexasRed, and CTxB when all three labels are present. Images shown depict the GUVs in their final state, i.e. with all labels present for a given condition. All scale bars are 5 µm.

It is possible that the labeling order (CTxB-Alexa647 first, EuTc second) may influence our observations. To determine if this is the case, we labeled DOPC/DPPC/cholesterol/GM1 (39.5:39.5:20:1) GUVs first with EuTc, followed by CTxB-Alexa647. We observed that EuTc

and CTxB-Alexa647 again colocalize (Fig. 6). In summary, we observe that regardless of labeling order, the EuTc colocalizes with CTxB-Alexa647. Furthermore, when all labels (TR-DHPE, CTxB-Alexa647, and EuTc) are present, all labels colocalize. However, when EuTc is not present, TR-DHPE and CTxB-Alexa647 do not colocalize. This suggests that upon the addition of EuTc, the CTxB-Alexa647 label, and thus the GM1, moves from the Lo phase to the Ld phase. Possible causes for our observations are that EuTc causes GM1 to prefer the Ld phase in phase-separated membranes and/or EuTc alters membrane order. We suspect that EuTc causes Ld membrane phases to become more ordered, which eliminates the preference of GM1 for the Lo phase.

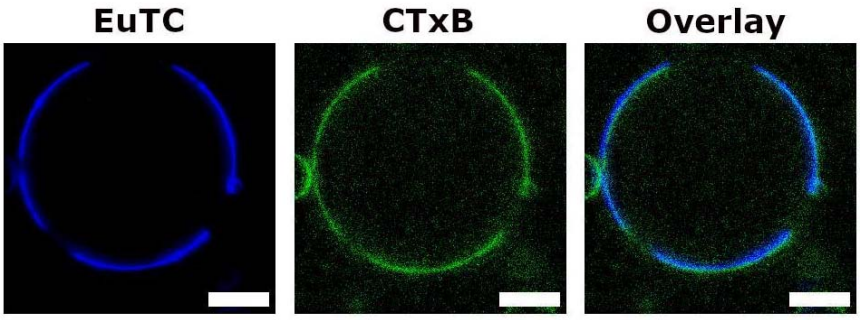

Figure 6. DOPC/DPPC/cholesterol/GM1 (39.5:39.5:20:1) GUVs were labeled with EuTc and then with CTxB-Alexa647. Labeling order (CTxB-Alexa647 then EuTc vs EuTc then CTxB-Alexa647) does not influence colocalization. All scale bars are 5 µm.

To examine the effects of EuTc on membrane order, we used fluorescence recovery after photobleaching (FRAP) to determine lipid diffusion coefficients. It is well established that increased membrane order causes the lipid diffusion coefficients to decrease. Based on our hypothesis, that EuTc causes Ld membrane phases to become more ordered, we anticipated that EuTc would reduce lipid diffusion in SLBs consisting of DOPC and different fluorescent probes, including TR-DHPE, TopFluorPC, and BODIPY-GM1. To analyze lipid diffusion and thereby

membrane order, we prepared supported lipid bilayers (SLBs) consisting of DOPC/TR-DHPE (99:1) and DOPC/TopFlourPC (99:1), and DOPC/BODIPY-GM1 (99:1). After SLB formation, FRAP recovery curves were collected before and after adding EuTc (1 μM) to the fluidic channels. As shown in Figure 7, with all compositions there is an obvious reduction in the rate of fluorescence recovery after EuTc incubation. The reduction in recovery rates translates to a significant reduction in lipid diffusion coefficients after EuTc exposure (Fig. 8). For example, with DOPC/TR-DHPE the diffusion coefficient drops from 1.67 ± 0.11 $\mu m^2/s$ to 0.55 ± 0.12 $\mu m^2/s$ after EuTc exposure, while with DOPC/TopFluorPC, the diffusion coefficient is reduced from 1.98 ± 0.08 $\mu m^2/s$ to 0.59 ± 0.08 $\mu m^2/s$. We chose the TR-DHPE and TopFluorPC probes for this experiment because their fluorescent moieties are linked to different parts of the phospholipid. The TR group of TR-DHPE is linked to the polar head group and exposed to the aqueous environment, and therefore may have more interaction with EuTc. On the other hand, the TopFluor group of TopFluorPC is linked to the hydrophobic tail. Lipid tail-linked TopFluor has been shown to reside deeply within the hydrophobic core of the bilayer.[30] Additionally, TopFluorPC presents the same phosphocholine headgroup as the background lipid DOPC.

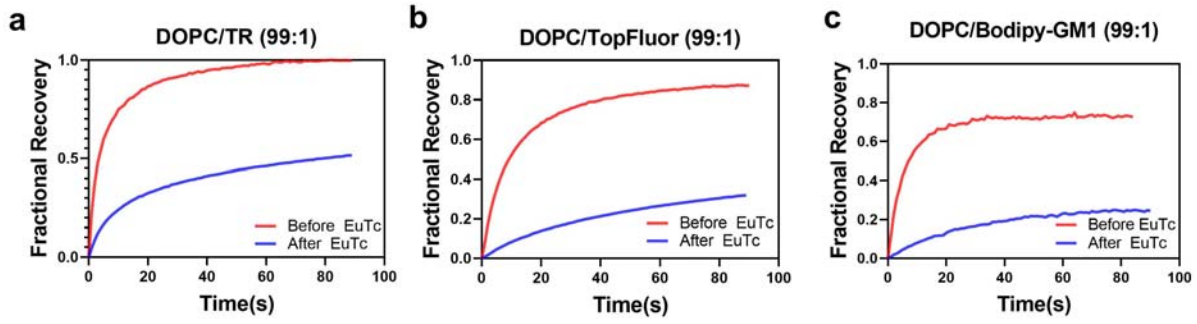

Figure 7. FRAP recovery curves of (a) DOPC/TR (99:1), (b) DOPC/TopFlourPC (99:1) and (c) DOPC/BODIPY-GM1 SLBs before EuTc exposure and after EuTc exposure.

Next, we wanted to determine if EuTc had an effect on the diffusion of GM1. To evaluate this, we utilized a fluorescent analog of GM1, BODIPY-GM1, and monitored its diffusion in DOPC bilayers. In SLBs consisting of DOPC/BODIPY-GM1 (99:1) we observed a similar reduction in recovery rates (Fig. 7c) and diffusion coefficients (Fig. 8b) after EuTc exposure when compared to the recovery rates and diffusion coefficients of DOPC/TR and DOPC/TopFlourPC. The DOPC/BODIPY-GM1 diffusion coefficient drops from 1.78 ± 0.25 $\mu m^2/s$ to 0.54 ± 0.07 $\mu m^2/s$ after the addition of EuTc. The fact that the diffusion coefficients after EuTc are comparable to those with TR-DHPE and TopFluorPC suggests that regardless of the probe employed, EuTc significantly reduces lipid diffusion. This indicates that EuTc's ability to decrease lipid diffusion is unlikely to arise from specific interactions between EuTc and GM1 or EuTc and the fluorescent probe, but rather stems from interactions with the background PC lipids in the bilayer, which may underlie the redistribution of GM1 observed in GUV imaging experiments.

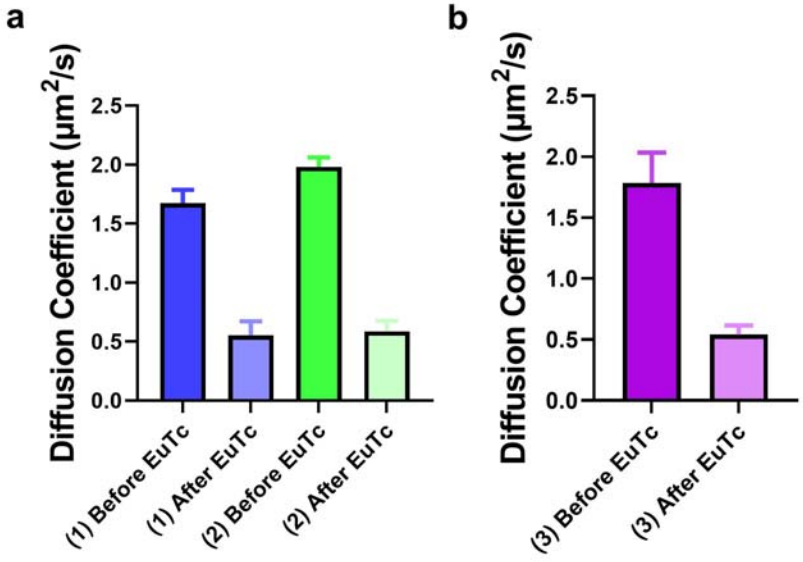

Figure 8. Influence of EuTc on lipid diffusion coefficients in SLBs. Diffusion coefficients for SLBs consisting of: (1) DOPC/TR (99:1), (2) DOPC/TopFlourPC (99:1) and (3) DOPC/BODIPY-GM1. Diffusion coefficients were measured using FRAP before and after EuTc

exposure and subsequent washout. Data is represented as mean ± standard deviation, N ≥ 9 for all samples.

3. CONCLUSIONS

In conclusion, this work demonstrates the application of a coordination complex probe suitable for imaging spatial heterogeneity of biomembranes. Compared to traditional organic probes for biomembranes, EuTc has a much narrower emission bandwidth, an extremely large Stokes shift, and a unique combination of excitation and emission wavelengths. Additionally, EuTc has a much longer emission lifetime (tens of μs)[13] than most organic membrane probes. These attractive properties suggest that EuTc may find applications in multicolor fluorescence and time-resolved imaging of biomembranes, with the caveat that some lipid redistribution may occur. We show that introducing EuTc to liposome suspensions results in a lipid concentration-dependent increase in EuTc luminescence. Additionally, when labeling phase separated GUVs with the EuTc complex, we observe a distinct contrast between Lo and Ld domains, where the EuTc labels the Ld domains. Surprisingly, labeling GM1-containing, phase-separating GUVs with EuTc results in GM1 losing its preference for the Lo phase. Our results demonstrate that EuTc alters membrane organization, and it is possible that tetracycline and its derivatives, when complexed with other more biologically relevant metal ions, may also alter the chemical and physical properties of lipid bilayer membranes. For example, tetracycline and derivatives in the presence of calcium have been shown to induce membrane invaginations, disrupt the spatial distribution of peripheral membrane proteins, and alter the size and distribution of regions of increased fluidity (RIFs) in gram-positive bacteria.[31] Furthermore, under physiological conditions free tetracycline concentrations are negligible, with Mg^{2+} and Ca^{2+} tetracycline complexes being the most prevalent forms.[32,33] Metal complexation of tetracycline decreases its bioavailability through altered interactions with gastrointestinal tract tissue.[34] Our results show

that EuTc interacts with biomembranes in a phase-sensitive manner and causes redistribution of certain lipids, which could potentially also occur with other Tc complexes *in vivo*.

4. METHODS

4.1 Reagents and Chemicals

Dioleoylphosphatidylcholine (DOPC), dipalmitoylphosphatidylcholine (DPPC), ganglioside GM1 (ovine brain), 1-palmitoyl-2-(dipyrromethene boron difluoride) undecanoyl-sn-glycero-3-phosphocholine (TopFluorPC) and cholesterol were all purchased from Avanti Polar Lipids (Alabaster, AL). Sucrose, chloroform, europium (III) chloride, tetracycline hydrochloride, and cholera toxin B subunit FITC conjugate (CTxB-FITC) were purchased from Sigma Aldrich. 3-(N-morpholino)propanesulfonic acid) (MOPS) was purchased from Acros Organics. Texas Red DHPE (TR-DHPE), BODIPY FL C_5-ganglioside GM1 (GM1-BODIPY) (Invitrogen), cholera toxin B subunit Alexa Fluor 647 tagged (CTxB-Alexa647), and sodium dodecyl sulfate (SDS) were purchased from ThermoFisher.

4.2 EuTc Preparation

In all experiments, EuTc was prepared by combining equimolar amounts of europium (III) chloride and tetracycline hydrochloride in 10 mM MOPS, pH 7.0. Prior to their combination, europium (III) chloride and tetracycline hydrochloride were kept as stock solutions in 10 mM MOPS, pH 7.0. The tetracycline hydrochloride stock solution was prepared fresh daily. The EuTc solutions, prepared fresh daily, typically contained 1 mM europium (III) chloride and 1 mM tetracycline hydrochloride. Unless otherwise stated, the EuTc solution was then diluted to 1 μM for spectroscopy and imaging. The EuTC complex was added to liposome and GUV samples after their preparation.

4.3 Liposome Preparation

Lipids dissolved in chloroform were mixed in glass vials to their desired molar ratios with a final concentration of 1.00 mg/mL. Chloroform was evaporated under vacuum at room temperature for a minimum of 2 h. Lipid films were rehydrated in MOPS buffer (10 mM MOPS, pH 7.00), vortexed and subjected to three freeze-thaw cycles. Freezing was accomplished by plunging the sample into liquid N_2 until frozen, and and then samples were thawed with a warm water bath. Liposomes were then extruded inside a mini-extruder (Avanti) using a 100 nm pore size polycarbonate membrane filter (Whatman) for a total of 23 passes. Immediately after, liposomes were used in fluorescence spectroscopy experiments and to form supported lipid bilayers (SLBs).

4.4 Preparation of GUVs

Giant unilamellar vesicles (GUVs) were made by electroformation.[32] Lipid mixtures were dried under vacuum, resuspended in chloroform, and then a droplet of lipid solution was transferred to clean indium tin oxide (ITO) coated slides (Delta Technologies, Loveland, CO). ITO slides were cleaned by swabbing the slides with 2% aqueous Alconox detergent solution and rinsing with MilliQ H_2O immediately thereafter, three times over. Lipid solutions on the ITO slides were dried under vacuum for a minimum of 15 min to remove chloroform. A capacitor was formed with a second ITO coated slide with a 0.3 mm Teflon spacer. The two slides were sandwiched together using binder clips. 400 µL of 200 mM sucrose was injected between the two slides. The total lipid concentration in the chamber was 1.0 mg/mL. GUVs were electroformed at 65 °C, using an AC signal with peak to peak amplitude of 3.0 V and frequency 10 Hz for 2 h (Siglent Technologies). GUVs were removed from the electroformation chamber and diluted 1:1000 with MOPS buffer in an Attofluor imaging chamber (ThermoFisher Scientific). Prior to imaging,

GUVs were exposed to 1 µM EuTc and/or 10 nM CTxB-Alexa647. A minimum of 30 GUVs among ≥ 3 individual preparations were examined for signal partitioning and representative images were chosen to produce in the figures.

4.5 Fluorescence Spectroscopy

Excitation and emission spectra were collected with a Fluorolog-2 Spectrofluorometer (HORIBA). Excitation spectra for EuTc were collected by scanning excitation from 350-450 nm while monitoring emission at 618 nm. EuTc emission spectra were collected from 560-700 nm by exciting at 400 nm. TR-DHPE excitation was collected by scanning from 450-605 nm while monitoring emission at 615 nm. Emission spectra for TR-DHPE were collected by scanning from 600-650 nm while exciting at 596 nm. EuTc (1 µM) emission was measured in the presence of DOPC (0.01 µM-100 µM) liposomes. TR-DHPE emission was measured from 1 µM DOPC liposomes containing 1 mol % TR-DHPE.

4.6 Fluorescence Microscopy

Glass coverslips were cleaned with 2 % (w/v) SDS solution and rinsed with ultrapure H_2O, and then dried with N_2 gas. Clean glass coverslips then underwent a UV-ozone treatment (UV/Ozone ProCleaner Plus, BioForce Nanosciences) for approximately 10 min. To label GUVs with EuTc and CTxB-Alexa647, they were first exposed to 1 µM EuTc, incubated for 5 min, then exposed to 10 nM CTxB-Alexa647 (or vice-versa), incubated for 5 min, and imaged immediately after. All imaging was done using an inverted microscope (Eclipse Ti, Nikon) equipped with a 100× oil immersion objective with a 1.49 numerical aperture. Fluorescence was excited using a LED light engine (Aura II, Lumencor), a Cy5 (Chroma), FITC (Chroma), TRITC (Chroma) or a

custom EuTc (Semrock) filter set. All images were captured with a 2048 × 2048 pixel sCMOS camera (Orca Flash 4.0 v2, Hamamatsu) controlled by Nikon Elements software.

4.7 Supported Lipid Bilayer Preparation for Fluorescence Recovery After Photobleaching (FRAP)

Glass coverslips were cleaned with 2% (w/v) SDS and rinsed with ultrapure H_2O and then dried with N_2 gas. The coverslip was subjected to a 10 min UV-ozone treatment and adhered to a self-adhesive bottomless 6-channel slide (Sticky-Slide VI 0.4, Ibidi). Vesicles to form SLBs contained either DOPC and 1 mol % GM1 or DOPC only with either 1 mol % TopFlourPC or 1 mol % TR-DHPE. The liposomes were diluted to 0.1 mg/mL in Tris buffer (10 mM Tris, 150 mM NaCl, pH = 7.0) and were injected into a channel of the sticky slide, and then incubated for 30 min. After incubation, excess liposomes were first washed out with Tris buffer, and then the buffer was exchanged for MOPS (pH = 7.0). After the SLBs were washed, they were imaged with an inverted microscope (Eclipse Ti, Nikon) equipped with a 100× oil immersion objective with a 1.49 numerical aperture. Fluorescence was excited using a LED light engine (Aura II, Lumencor), a FITC or TRITC filter set (Chroma) and images were captured with 2048 × 2048 pixel sCMOS camera (Orca Flash 4.0 v2, Hamamatsu). Each sample was photobleached using a 405 nm laser (50 mW) pulse for 2 s, and fluorescence recovery was captured at 1 s intervals for 60 s. After FRAP, the samples were exposed to 1 µM EuTc, incubated for 1 h and photobleached again. Recovery was monitored and recorded for 1 s intervals for 60 s and captured using a TRITC or FITC filter set. Lipid diffusion coefficients and mobile fractions were calculated using the Hankel transformation and MATLAB code provided by Jonsson et al.[33]

Data Availability

The datasets generated during and/or analyzed during the current study are available from the corresponding author on reasonable request.

References

[1] D. Lingwood, K. Simons, *Science* **2010**, *327*, 46.
[2] S. L. Veatch, S. L. Keller, *Biophys J* **2003**, *85*, 3074.
[3] T. E. Thompson, T. W. Tillack, *Annu Rev Biophys Biophys Chem* **1985**, *14*, 361.
[4] A. S. Klymchenko, R. Kreder, *Chem Biol* **2014**, *21*, 97.
[5] T. Baumgart, G. Hunt, E. R. Farkas, W. W. Webb, G. W. Feigenson, *Biochim Biophys Acta* **2007**, *1768*, 2182.
[6] J.-C. G. Bünzli, *Chem Rev* **2010**, *110*, 2729.
[7] L. N. Krasnoperov, S. A. E. Marras, M. Kozlov, L. Wirpsza, A. Mustaev, *Bioconjug Chem* **2010**, *21*, 319.
[8] C. N. Antonio, P. M. Grazia, C. Marialessandra, B. Francesco, P. Roberto, *Met Based Drugs* **2007**, *2007*, 12635.
[9] L. C. Courrol, A. M. Monteiro, F. R. O. Silva, L. Gomes, N. D. Vieira, M. A. Gidlund, A. M. F. Neto, *Opt Express* **2007**, *15*, 7066.
[10] M. Wu, Z. Lin, O. S. Wolfbeis, *Anal Biochem* **2003**, *320*, 129.
[11] M. A. Alcala, C. M. Shade, H. Uh, S. Y. Kwan, M. Bischof, Z. P. Thompson, K. A. Gogick, A. R. Meier, T. G. Strein, D. L. Bartlett, R. A. Modzelewski, Y. J. Lee, S. Petoud, C. K. Brown, *Biomaterials* **2011**, *32*, 9343.
[12] L. M. Hirschy, E. V. Dose, J. D. Winefordner, *Analytica Chimica Acta* **1983**, *147*, 311.
[13] L. M. Hirsch, T. F. Van Geel, J. D. Winefordner, R. N. Kelly, S. G. Schulman, *Anal Chim Acta* **1985**, *166*, 207.
[14] M. Schäferling, D. B. M. Grögel, S. Schreml, *Microchim Acta* **2011**, *174*, 1.
[15] M. P. Lowe, D. Parker, *Chem Commun* **2000**, 707.
[16] A. Beeby, I. M. Clarkson, R. S. Dickins, S. Faulkner, D. Parker, L. Royle, A. S. de Sousa, J. A. G. Williams, M. Woods, *J Chem Soc, Perkin Trans 2* **1999**, *0*, 493.
[17] Y. Rakicioglu, J. H. Perrin, S. G. Schulman, *J Pharm Biomed Anal* **1999**, *20*, 397.
[18] O. Alptürk, O. Rusin, S. O. Fakayode, W. Wang, J. O. Escobedo, I. M. Warner, W. E. Crowe, V. Král, J. M. Pruet, R. M. Strongin, *Proc Natl Acad Sci USA* **2006**, *103*, 9756.
[19] L. dos S. Teixeira, A. N. Grasso, A. M. Monteiro, A. M. F. Neto, N. D. Vieira, M. Gidlund, J. Steffens, L. C. Courrol, *J Fluoresc* **2011**, *21*, 887.
[20] R. D. Jee, *Analyst* **1995**, *120*, 2867.
[21] O. S. Wolfbeis, A. Dürkop, M. Wu, Z. Lin, *Angew Chem Int Ed* **2002**, *41*, 4495.
[22] S. Pandya, J. Yu, D. Parker, *Dalton Trans.* **2006**, 2757.
[23] K. Binnemans, *Coord Chem Rev* **2015**, *295*, 1.
[24] C. Dietrich, L. A. Bagatolli, Z. N. Volovyk, N. L. Thompson, M. Levi, K. Jacobson, E. Gratton, *Biophys J* **2001**, *80*, 1417.
[25] B. L. Stottrup, D. S. Stevens, S. L. Keller, *Biophys J* **2005**, *88*, 269.
[26] G. M. Kuziemko, M. Stroh, R. C. Stevens, *Biochemistry* **1996**, *35*, 6375.
[27] K. Simons, R. Ehehalt, *J Clin Invest* **2002**, *110*, 597.
[28] T. Williams, A. Jenkins, *J Am Chem Soc* **2008**, *130*, 6438.

[29] B. Westerlund, J. P. Slotte, *Biochim Biophys Acta* **2009**, *1788*, 194.
[30] J. G. Kay, M. Koivusalo, X. Ma, T. Wohland, S. Grinstein, *MBoC* **2012**, *23*, 2198.
[31] M. Wenzel, M. P. Dekker, B. Wang, M. J. Burggraaf, W. Bitter, J. R. T. van Weering, L. W. Hamoen, *Commun Biol* **2021**, *4*, 1.
[32] G. Berthon, M. Brion, L. Lambs, *J Inorg Biochem* **1983**, *19*, 1.
[33] M. Brion, G. Berthon, J.-B. Fourtillan, *Inorg Chim Acta* **1981**, *55*, 47.
[34] P. J. Neuvonen, *Drugs* **1976**, *11*, 45.

Acknowledgements

N.J.W. acknowledges funding from Lehigh University and the National Science Foundation (Award Number 2044792).

Author Contributions

J.L.C., A.I.M., A.R.H-S., and N.J.W. designed experiments, J.L.C. carried out the experiments; J.L.C., A.R.H-S., and N.J.W. analyzed the data; J.L.C. and N.J.W. wrote the manuscript with input from all co-authors.

Competing Interests

The authors declare that they have no known competing financial interests or personal relationships that could have appeared to influence the work reported in this paper.

Supplementary Information

Supplementary material contains custom filter cube characteristics and additional images of GUVs labeled with EuTc, TR-DHPE, and CTxB-FITC.